Journal of Materials Chemistry A

PAPER

View Article Online
View Journal | View Issue

Cite this: J. Mater. Chem. A, 2014, 2, 5738

Electrosprayed PLGA smart containers for active anti-corrosion coating on magnesium alloy AMlite†

Jing-Yu Chen,[a] Xiao-Bo Chen,*[bc] Jing-Liang Li,[a] Bin Tang,[a] Nick Birbilis[bc] and Xungai Wang*[a]

Received 3rd December 2013
Accepted 5th February 2014

DOI: 10.1039/c3ta14999d

www.rsc.org/MaterialsA

A novel self-healing system, consisting of poly(lactic-*co*-glycolic) acid (PLGA) porous particles loaded with a corrosion inhibitor, *i.e.* benzotriazole (BTA), has been successfully achieved *via* direct electro-spray deposition and subsequent epoxy spraying upon magnesium (Mg) alloy AMlite. The two-step process greatly simplified the multi-step fabrication of smart coatings reported previously. The PLGA particles demonstrate rapid response to both water and pH increase incurred by corrosion of Mg, ensuring instant and ongoing release of BTA to self-heal the protective functionality and retard further corrosion. Furthermore, nanopores in the PLGA–BTA microparticles, formed by the fast evaporation of dichloromethane during the electrospray process, also contribute to the fast release of BTA. Using Mg alloy AMlite as a model substrate which requires corrosion protection, potentiodynamic polarisation characterisation and scratch testing were adopted to reveal the anti-corrosion capability of the active coating.

Introduction

The past decade has witnessed significant efforts in addressing the global metallic corrosion challenge, with a focus on avoiding or mitigating the huge economic losses incurred by corrosion[1–14] and on the development of protective coatings for metals. Hitherto, one of the most effective routes to provide satisfactory corrosion protection for metals is the use of chromate conversion coatings.[15] The outstanding performance of chromate-based coatings originates from their high stability (barrier role) and self-healing nature (active role). When corrosion occurs, hexavalent chromium ions are reduced to trivalent chromium oxide, which is highly insoluble and stable in corrosive media. However, the hexavalent chromium species can cause DNA damage and cancer, which hinders their continued application.[16] Thus it is imperative to develop protective coatings with performance comparative to that of chromate, *i.e.* with a self-healing characteristic.[17,18]

Many protective coatings have been developed with the aim of chromate replacement.[15,17] Most of those coatings, however, provide a barrier function only, which means that the protection will disappear when they are damaged/or lose integrity. To prolong the lifespan of metallic components under harsh conditions (*e.g.*, marine, humid environment), researchers have turned their interests to active coatings, combining both passive functionality (*e.g.*, barrier, color, adhesion) and self-healing property, *i.e.* a rapid/active feedback against changes in a local environment.[18] In general, an active coating is composed of a matrix of a traditional coating material with smart micro- or nanosized containers embedded inside. When the coating is damaged (*e.g.*, mechanical scratching or pitting corrosion), the containers are stimulated/triggered to release functional agents (*e.g.*, paint precursor or corrosion inhibitors) to provide a prolonged lifespan to the underlying metal.

In active coatings, the response of smart containers to a certain stimulus, plays a critical role in achieving high protection efficiency. For example, polymer micro-containers of polyurethane or urea-formaldehyde with an encapsulated fluid agent were reported.[7–11] When the coating layer was cracked, the containers were broken/melted to release the functional agent to form a protective layer on the metal surface. The size of the micro-containers has to be sufficiently large, for example, tens of micrometers, to realise fast release while the containers were mechanically damaged. This limits their applications since very thick coatings are needed to contain these containers. To tackle this technical issue, smaller containers were developed for thinner coatings, such as coatings *via* the sol–gel technique.[3–5,19,20] The release from these containers, however, could not be triggered by mechanical damage, since they were too small to be broken. In this context, release triggered by pH increase is of current interest for corrosion protection owing to the fact that the pH value in the vicinity of the surface of the

[a]Institute for Frontier Materials, Deakin University, Waurn Ponds, Victoria 3217, Australia. E-mail: xungai.wang@deakin.edu.au

[b]Department of Materials Engineering, Monash University, Clayton, VIC 3800, Australia. E-mail: xiaobo.chen@monash.edu

[c]The ARC Centre of Excellence for Design in Light Metals, Monash University, Clayton, VIC 3800, Australia

† Electronic supplementary information (ESI) available. See DOI: 10.1039/c3ta14999d

metal increases when corrosion occurs electrochemically in an aqueous environment. For example, layer-by-layer (LBL) polyelectrolyte nanoparticles loaded with an inhibitor were prepared for pH-triggered release.[5,20] The spheres-containing sol–gel layer showed enhanced corrosion protection; however, the process for producing LBL particles remains complicated. Additionally, some inorganic materials such as halloysite nanotubes and porous silica nanoparticles have also been fabricated and loaded with inhibitors and applied as containers.[2–4,13,14] Nonetheless, the release rate is low since it relies mainly on the molecular diffusion from the pores of the containers to the environment. Therefore it will be more practical if the containers are degradable in water which can provide a rapid response to coating damage, since corrosion nominally takes place in aqueous environments. This, along with the subsequent pH increase which accompanies the cathodic half-reaction of corrosion, will greatly enhance the release of corrosion inhibiting agents to the metal surface.

Poly(lactic-*co*-glycolic) acid (PLGA) has been extensively used in controlled drug delivery, which degrades by hydrolysis of its ester linkages when exposed to water.[21–23] Herein, unlike existing regular uses of this polymer, an innovative active coating was fabricated consisting of a PLGA smart container loaded with inhibitor benzotriazole (BTA) *via* the electrospray process, and the capability of the coating to inhibit corrosion was tested on magnesium (Mg) alloy AMlite. When the painting is damaged, water in contact with the PLGA containers induces reliable and long lasting release of the inhibitor. As indicated by the enhanced release in solution with a higher pH,[24] the *in situ* release could be enhanced by a pH increase induced by metal corrosion. Compared to the solely pH triggered release of the smart containers reported previously, the dual stimuli (water and pH) triggered release is more practically significant. By using fast evaporating dichloromethane (DCM) as a solvent, the hierarchical structure of microparticles with nanopores on the surface was obtained during the electrospray process,[25] which further accelerated the inhibitor release, resulting in improvement in protection.

An additional advantage of the present work is the simplified preparation process *via* the electrospray process. Electrospraying is an electro-dynamic process in which droplets of a polymer solution are formed in an electric field under a high voltage in a short distance. During the spray process, the solvent evaporates and micro- or nanoparticles of a polymer can be obtained in the ground electrode, which is usually a metal plate.[26–28] In the previous reports, the fabrication of active coating was composed of multiple steps, *e.g.* smart container fabrication, inhibitor loading, dispersing containers in coating materials, and applying coating on the metal surface. In this work, the electrospray process was used to produce the inhibitor-loaded containers and to deposit them on the metal surface in one step. Epoxy paint was then sprayed to cover the containers. Furthermore, since the smart containers were directly applied on the metal, there is no need to consider their dispersion in coating materials. This means that their applications are not restricted by the coating materials.

Experimental

Preparation of protective coatings on Mg alloy AMlite flakes

A weighed amount of PLGA (Lactel®, Mw 40–75k) and BTA were dissolved in 1 ml DCM. Different samples were obtained by varying the concentration of PLGA (5–20 wt%) and the loading ratio of BTA to PLGA (10–20 wt%). The solution was magnetically stirred for 30 min at room temperature in a sealed vial. Then it was electro-sprayed from a syringe at 20 kV with a distance (from the tip of needle to the collector) of 20 cm, and the flow rate was 1 ml min^{-1}. A piece of Al foil was used as the opposite electrode. The PLGA–BTA particles were collected on commercial die-cast Mg alloy AMlite flakes (1 cm^2 each, Magontec Ltd. Pty.) which were fixed on the centre of the Al foil. The collecting time was fixed strictly to 2 min for all the samples. Subsequent epoxy painting (White Knight®, epoxy enamel, white color) was applied on the metal flakes by spray. The samples were dried at room temperature in a fume hood for 3 days.

Characterisation

Scanning electron microscopes (FEG-SEM Zeiss Supra 55VP and Jeol NeoScope JCM-5000) were applied in the morphology study of the PLGA–BTA microcontainers. The encapsulation of BTA into PLGA microparticles was proven by Fourier Transform Infrared Spectroscopy-Attenuated Total Reflectance (FTIR-ATR) measurement with a Bruker Vertex 70 FTIR spectrometer. The surface coverage of Mg alloy flakes with PLGA–BTA were quantified by analysing SEM images with an ImageJ software. The surface roughness of the various coated Mg alloy AMlite specimens was analysed with a VECCO WYKO NT1100 optical profilometer.

BTA release profile

To evaluate the release kinetics, a thick layer of PLGA–BTA microparticles was collected for 1 h on small pieces of silicon wafer (around 4 cm^2). The releasing tests were carried out in deionised water and NaOH–$Na_2B_4O_7$ buffer (pH = 10) respectively. The concentration of BTA was analysed by UV-Vis spectrometry (Varian Cary 3E) in the wavelength region of 200–800 nm.

Electrochemical testing

Electrochemical tests employed a flat-cell (PAR), which contained approximately 300 ml 0.1 M NaCl: 1 cm^2 of specimen area was exposed. The sample prepared from 15 wt% PLGA solution with 20 wt% BTA loading was the working electrode, and a saturated calomel reference electrode (SCE), together with a Ti mesh counter electrode were used. Open circuit potential (OCP), potentiodynamic polarisation and electrochemical impedance spectroscopy (EIS) tests were performed using a Biologic VMP-3Z potentiostat. Specimens were allowed to stabilise for 10 min to reach a sufficiently stable OCP, prior to polarisation at a rate of 1 mV s^{-1}. The impedance measurements were carried out at OCP with applied 10 mV sinusoidal

perturbation in a 100 kHz down to 10 mHz frequency range with 10 steps per decade at room temperature in a Faraday cage. The corrosion current density (i_{corr}) values were determined using a Tafel-type extrapolation of the polarisation curve carried out with EC-Lab software V10.35 (Biologic). At least three samples prepared under the same conditions were tested in order to ensure reproducibility of the results.

Results and discussion

PLGA–BTA particles produced by the electrospray process

The influences of PLGA concentration and ratio of BTA to PLGA on the size and morphology of the particles produced were investigated with BTA to PLGA fixed at 20 wt%, as shown in Fig. 1. A range of PLGA concentrations from 20 wt% to 5 wt% were examined. At the PLGA concentration of 20 wt%, "bead" fibers were obtained (Fig. 1a). The production of bead fibres at high concentrations has also been reported by other researchers.[29] Reducing the concentration to 15 wt%, PLGA particles with perfect spherical shape could be achieved (Fig. 1b). The diameters of most of these spheres were around 5 μm, while there were also some smaller particles with diameters as low as 1 μm. At the same time, a very small amount of fibers can be seen among the products. When the concentration was reduced to 10 wt%, irregularly shaped spheres were the main products (Fig. 1c), attributing to the balance between polymer chain entanglement and Coulomb fission occurring inside the droplets in a high electro field.[28] When the concentration was further reduced to 5 wt%, although spherical particles were obtained, the particles were quite flat. It might be due to the large amount of solvent DCM. When the particles hit the collector, the solvent did not evaporate completely, resulting in particle deformation.

On the PLGA particles, the secondary structure was constructed by selecting DCM as a solvent for the electrospray process, which is of very high evaporation speed. From the inset images with higher magnification in Fig. 1B and D it can be seen that the surface of particles was covered with a large amount of pores of around tens of nanometers in diameter. The pores on particles prepared with a 5 wt% PLGA solution were larger than those on the particles prepared with a 15 wt% PLGA solution.

The influences of BTA contents on the morphologies of final products were also studied, with the concentration of PLGA fixed at 20 wt%. PLGA particles with BTA loading ratios of 20%, 15% and 10% were prepared, as shown in Fig. 1B, E and F. The results indicate that the loading ratio of BTA did not have obvious impact on the morphology of particles.

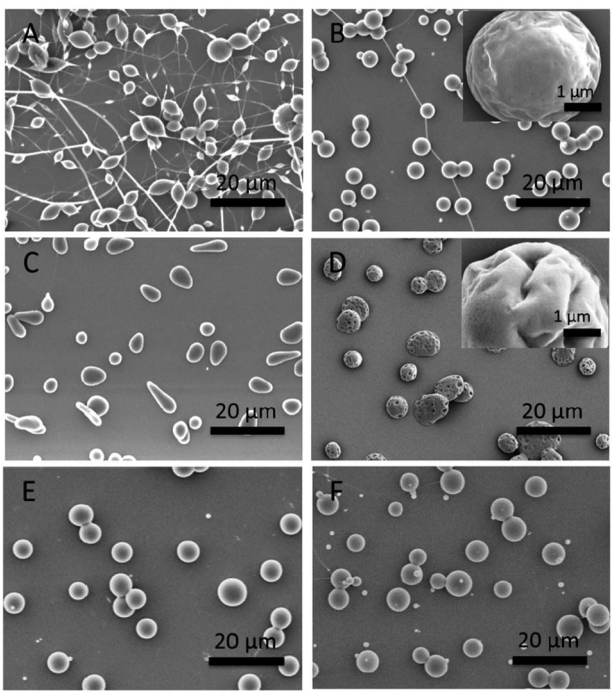

Fig. 1 SEM images of PLGA–BTA particles. (A–D): prepared from DCM solutions with different PLGA concentrations: (A) 20 wt%; (B) 15 wt%; (C) 10 wt%; (D) 5 wt%. The ratio of BTA to PLGA was fixed at 20%. (E) and (F) prepared from 15% PLGA solution with different BTA loading ratios to PLGA: (E) 15%; (F) 10%.

FTIR

The FTIR-ATR spectra of PLGA, BTA and electrosprayed PLGA–BTA composite particles are shown in Fig. 2. The peaks at 1747 and 1083 cm^{-1} are due to the stretching vibration of C=O and C–O in PLGA, respectively. Those at 1203, 740, and 775 cm^{-1} can be assigned to the aromatic ring in BTA. All these characteristic peaks are present in the spectra of electrosprayed particles, indicating the successful incorporation of BTA into the PLGA particles.

Controlling the density of PLGA–TBA particles on the surface of metal flakes

The density of PLGA–BTA microparticles, deposited on the surface of metal flakes, could be controlled by varying the collection time. Ten spots on each sample were selected randomly to evaluate the density of microparticles at a certain time. When the collecting time was 1 min, PLGA spheres occupied around 16.45% of the flake surface. While when it

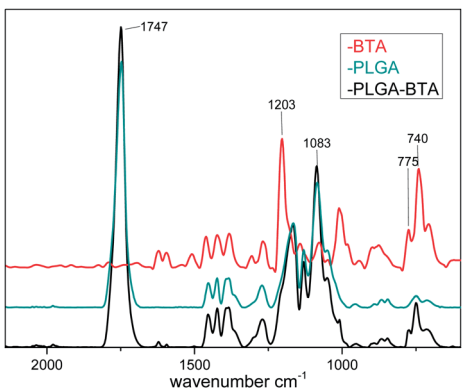

Fig. 2 FTIR-ATR spectra of BTA, PLGA and electrosprayed PLGA–BTA particles.

reached 3 min, around 20% of the surface was covered. When the collecting time was prolonged to, for example, 6 min, a significant overlap of particles was observed. Therefore, surface coverage at longer collection times was not evaluated.

Release of BTA

The degradation processes in an aqueous environment of pH 7 and 10 of PLGA–BTA microparticles on a silica wafer were investigated by SEM, as shown in Fig. 3A–F. At a high pH value (10), it is evident that the structure of the particles collapsed in basic buffer. After 48 h, only a small amount of residual particles can be found on the substrates, containing a large cavity in the middle and a smaller diameter than that of the original ones. At a pH value of 7, no collapse occurred but some pores on the surface developed.

The release kinetics of BTA from PLGA microcontainers determines the protecting efficiency of an active coating. As shown in Fig. 3g, in an aqueous environment of pH = 7, all samples showed higher speed of BTA release when exposed to water, a burst release was observed within 0.5 h, which ensured the formation of a protective layer instantly on the metal surface when coating damage appeared. After that, the release slowed down, lasting for more than 48 h. Since metal corrosion usually leads to pH increase, BTA release in a pH = 10 environment was also tested. All samples exhibited an enhanced releasing rate at this higher pH because of the faster degradation of PLGA in the aqueous environment of higher pH.[24] The pH enhanced release will definitely bring about an additional benefit in improving the protective function of the active coating. PLGA has been extensively used for controlled release. In that case, advantage is taken of its degradation in a slightly acidic environment. However, its degradation is faster under alkaline conditions,[24] which has not been utilised for controlled release. This work demonstrates for the first time that this feature is useful for protective coatings. It is also worth mentioning that although burst release is not desired in controlled drug delivery,[30–32] it would be an advantage for corrosion protection as fast deposition of inhibitor molecules ensures quicker mitigation of the electrochemical reactions on the metal surface.

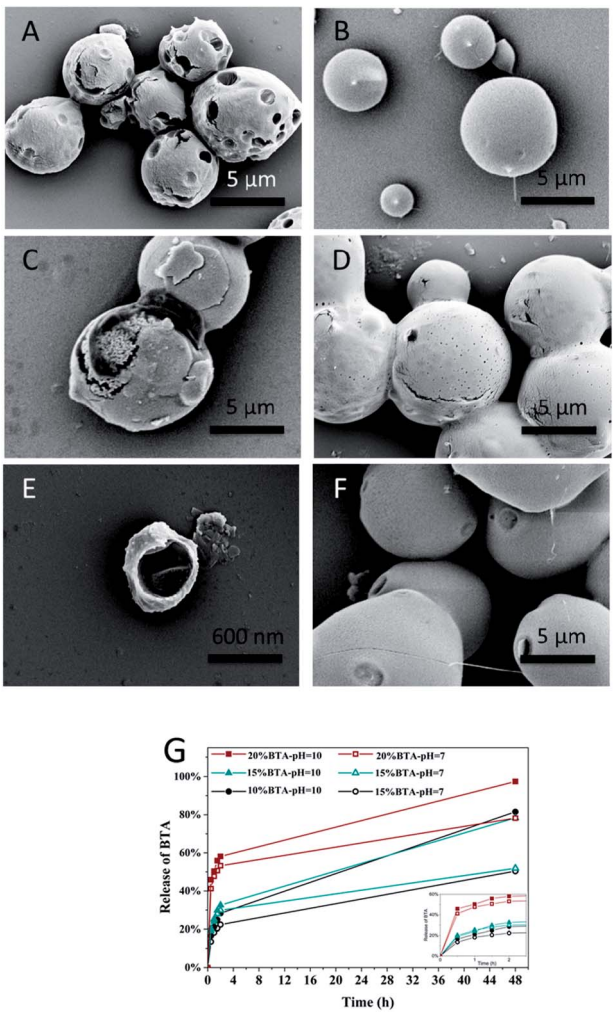

Fig. 3 A–F) SEM images of PLGA–BTA microparticles in a pH = 10 (A, C and E) and pH = 7 (B, D and F) environment after 8 h, 24 h, and 48 h. (G) BTA release profile in a pH = 7 and pH = 10 environment in 48 h. The inset shows the burst release for the first 2 h.

Electrochemical analysis

Potentiodynamic polarisation was conducted to assess the general protective characteristics of the active coating in relation to a standard as-cast AMlite specimen (Fig. 4a). The as-cast AMlite displayed a corrosion potential (E_{corr}) of ~ -1597 mV_{SCE} and a corrosion current density (i_{corr}) of 4.0×10^{-6} A cm^{-2}. It is apparent that there exists a pseudo-passive region prior to breakdown of protection and the subsequent onset of localised corrosion, which can be attributed to the presence of a partially protective oxide/hydroxide film on Mg alloys. The native surface film easily transforms/dissolves into soluble $MgCl_2$ upon exposure to NaCl containing the electrolyte and thus the passive/protective function is jeopardised. Applying BTA–PLGA nanoparticles onto the AMlite surface disrupted the continuity of the oxide film and mitigated the limited protective feature, though the E_{corr} (-1529 mV_{SCE}) increased and i_{corr} (3.0×10^{-6} A cm^{-2}) decreased slightly. A low current is maintained over a large range of potentials in the case of epoxy spray-painted specimens, concomitant with the barrier effect which is persistent to potentials of ~ -1400 mV_{SCE}. With regards to the epoxy coating containing BAT–PLGA particles, it can be seen that a broader range of potentials related to a low current was realised, with estimates of a free corrosion rate, i_{corr}, in the range of $\sim 2 \times 10^{-8}$ A cm^{-2}. The 'passive' region was compromised at anodic potentials $> \sim -1150$ mV_{SCE}. What is, however, interesting to note, is that when the coating breakdown was realised, and localised corrosion proceeds, there is fluctuation in the measured current that is associated only with the epoxy coating containing BAT–PLGA particle specimens, indicating that currents are periodically restricted perhaps due to the ongoing release of the BTA inhibitor from PLGA containers. Whilst the polarisation experiments provide a mechanistic basis, physical testing is also essential for probing if the self-healing property was realised on AMlite *via* applying the BTA–PLGA system.

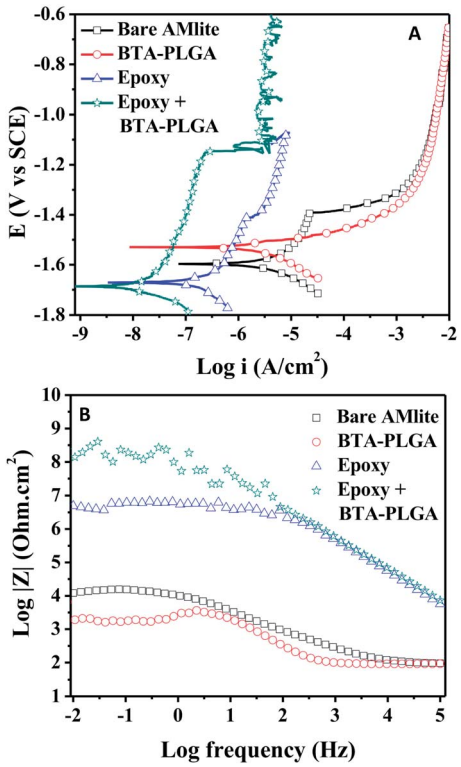

Fig. 4 Pontentiodynamic polarisation curves (A) and EIS spectra (Bode mode, B) of as-cast AMlite (black square) and three different coatings (BTA–PLGA particles only, red circle; Epoxy paint only, blue triangle; and Epoxy containing BTA–PLGA particles, green star) in 0.1 M NaCl electrolyte. The PLGA particles were prepared from 15 wt% solution with 20 wt% BTA loading.

The EIS was also used to estimate corrosion protection of the different coatings. The low frequency impedance is dependent on the nature of the coatings. The EIS spectrum of the Mg alloy AMlite coated with epoxy containing BTA–PLGA nanocontainers displays the highest impedance value (above 10^8 ohm cm^2) at low frequencies, indicating the best corrosion protection.

As such, to further demonstrate the protective function of the PLGA microcontainers, scratched specimens coated with epoxy and both without and with PLGA microcontainers were immersed in 0.1 M NaCl electrolyte for 30 min. Micrographs (Fig. 5) demonstrate that the entire scratched region of the paint without BTA–PLGA particles was corroded severely. At higher magnification, it is apparent that a number of cracks were present, which was the corrosion products from the 30 min immersion in NaCl. Without the corrosion inhibitor, peeling off the protective epoxy paint led to exposure of metallic Mg AMlite to the corrosive medium and gave rise to continuous corrosion. In terms of the painting with PLGA–BTA, it can be seen that only one spot was corroded as severely as the paint without the corrosion inhibiting agent. Whilst the other regions were as intact as that prior to immersion in NaCl, which was attributed to the inhibiting role of BTA released from PLGA containers when pH increased incurred by corrosion.

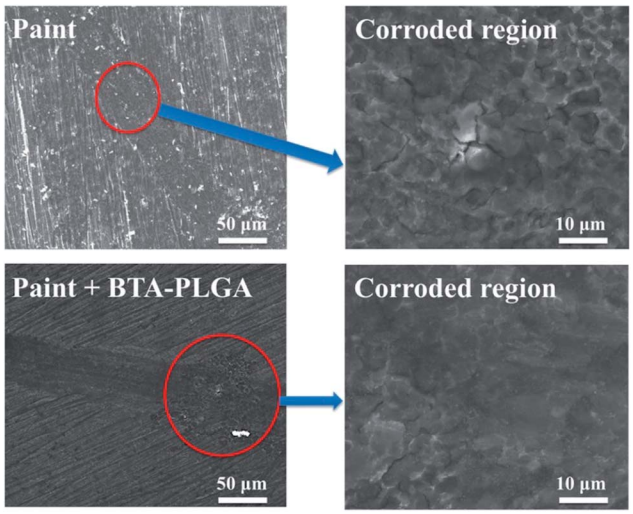

Fig. 5 SEM micrographs of the scratched marks and corroded regions of paints with and without BTA–PLGA microparticles prepared with 15 wt% solution with 20% BTA loading.

The long term stability of the PLGA–BTA/epoxy coating on AMlite flakes was studied by the preleaching test. After immersion in water for 18 days, no BTA was detected in water and the coating layer was intact. The surface roughness of the hybrid coating was also investigated, indicating that the PLGA–BTA microparticles have no influence on the epoxy coating.

Conclusions

Nanoporous PLGA microparticles loaded with the BTA inhibitor were prepared *via* the electrospray process and applied as smart containers for active anticorrosion epoxy coating. The BTA loading rate can reach as high as 20 wt%. Additionally, fast and continuous release of BTA can be realised for the nanopores on the PLGA–BTA microparticles. Furthermore, comparing with the traditional epoxy coating, the as-prepared active coating exhibits enhanced anti-corrosion ability judged by potentiodynamic polarisation and scratch testing on Mg alloy AMlite. Most importantly, our method can greatly reduce the complex steps previously reported for active coatings into two simple steps: electrospraying and deposition of inhibitor-loaded containers on Mg alloys, followed by epoxy paint coating.

Acknowledgements

X. C. and N. B. gratefully acknowledge the financial support by the ARC Centre of Excellence for Design in Light Metals *via* the Seed Grant Scheme.

Notes and references

1 A. Latnikova, D. Grigoriev, M. Schenderlein, H. Möhwald and D. Shchukin, *Soft Matter*, 2012, **8**, 10837–10844.
2 M. J. Hollamby, D. Fix, I. Donch, D. Borisova, H. Mohwald and D. Shchukin, *Adv. Mater.*, 2011, **23**, 1361–1365.

3 D. Borisova, H. Möhwald and D. G. Shchukin, *ACS Nano*, 2011, **5**, 1939–1946.
4 D. Fix, D. V. Andreeva, Y. M. Lvov, D. G. Shchukin and H. Möhwald, *Adv. Funct. Mater.*, 2009, **19**, 1720–1727.
5 D. G. Shchukin, M. Zheludkevich, K. Yasakau, S. Lamaka, M. G. S. Ferreira and H. Möhwald, *Adv. Mater.*, 2006, **18**, 1672–1678.
6 S. Neema, M. Selvaraj, J. Raguraman and S. Ramu, *J. Appl. Polym. Sci.*, 2013, **127**, 740–747.
7 M. Huang and J. Yang, *J. Mater. Chem.*, 2011, **21**, 11123–11130.
8 S. J. García, H. R. Fischer, P. A. White, J. Mardel, Y. González-García, J. M. C. Mol and A. E. Hughes, *Prog. Org. Coat.*, 2011, **70**, 142–149.
9 R. S. Jadhav, D. G. Hundiwale and P. P. Mahulikar, *J. Appl. Polym. Sci.*, 2011, **119**, 2911–2916.
10 C. Suryanarayana, K. C. Rao and D. Kumar, *Prog. Org. Coat.*, 2008, **63**, 72–78.
11 A. Pilbáth, T. Szabó, J. Telegdi and L. Nyikos, *Prog. Org. Coat.*, 2012, **75**, 480–485.
12 D. G. Shchukin, *Polym. Chem.*, 2013, **4**, 4871–4878.
13 D. Borisova, D. Akçakayıran, M. Schenderlein, H. Möhwald and D. G. Shchukin, *Adv. Funct. Mater.*, 2013, **23**, 3799–3812.
14 D. Borisova, H. Moehwald and D. G. Shchukin, *ACS Appl. Mater. Interfaces*, 2012, **4**, 2931–2939.
15 J. E. Gray and B. Luan, *J. Alloys Compd.*, 2002, **336**, 88–113.
16 R. Saha, R. Nandi and B. Saha, *J. Coord. Chem.*, 2011, **64**, 1782–1806.
17 X. B. Chen, N. Birbilis and T. B. Abbott, *Corrosion*, 2011, **67**, 0350051–03500516.
18 D. G. Shchukin and H. Mohwald, *Chem. Commun.*, 2011, **47**, 8730–8739.
19 D. O. Grigoriev, K. Köhler, E. Skorb, D. G. Shchukin and H. Möhwald, *Soft Matter*, 2009, **5**, 1426–1432.
20 M. L. Zheludkevich, D. G. Shchukin, K. A. Yasakau, H. Möhwald and M. G. S. Ferreira, *Chem. Mater.*, 2007, **19**, 402–411.
21 R. C. Mundargi, V. R. Babu, V. Rangaswamy, P. Patel and T. M. Aminabhavi, *J. Controlled Release*, 2008, **125**, 193–209.
22 C. Wischke and S. P. Schwendeman, *Int. J. Pharm.*, 2008, **364**, 298–327.
23 H. K. Makadia and S. J. Siegel, *Polymers*, 2011, **3**, 1377–1397.
24 C. C. Chu, *J. Biomed. Mater. Res.*, 1982, **16**, 117–124.
25 J. Zheng, H. Zhang, Z. Zhao and C. C. Han, *Polymer*, 2012, **53**, 546–554.
26 M. Cloupeau and B. Prunet-Foch, *J. Aerosol Sci.*, 1994, **25**, 1021–1036.
27 B. Almeria, T. M. Fahmy and A. Gomez, *J. Controlled Release*, 2011, **154**, 203–210.
28 B. Almeria, W. Deng, T. M. Fahmy and A. Gomez, *J. Colloid Interface Sci.*, 2010, **343**, 125–133.
29 L. Tong, W. Hongxia, W. Huimin and W. Xungai, *Nanotechnology*, 2004, **15**, 1375–1381.
30 S. D. Allison, *Expert Opin. Drug Delivery*, 2008, **5**, 615–628.
31 Y. Yamaguchi, M. Takenaga, A. Kitagawa, Y. Ogawa, Y. Mizushima and R. Igarashi, *J. Controlled Release*, 2002, **81**, 235–249.
32 A. L. Silva, R. A. Rosalia, A. Sazak, M. G. Carstens, F. Ossendorp, J. Oostendorp and W. Jiskoot, *Eur. J. Pharm. Biopharm.*, 2013, **83**, 338–345.